Environmental Pollution 255 (2019) 113124

Contents lists available at ScienceDirect

Environmental Pollution

journal homepage: www.elsevier.com/locate/envpol

Transport and retention of engineered silver nanoparticles in carbonate-rich sediments in the presence and absence of soil organic matter☆

Yorck F. Adrian [a], Uwe Schneidewind [a, b], Scott A. Bradford [c, *], Jirka Šimůnek [d], Erwin Klumpp [e], Rafig Azzam [a]

[a] Department of Engineering Geology and Hydrogeology, RWTH Aachen University, Lochnerstr. 4-20, 52064 Aachen, Germany
[b] Department of Civil and Environmental Engineering, Western University, London, ON N6A3K7, Canada
[c] US Salinity Laboratory, USDA, ARS, Riverside, CA 92507, USA
[d] Department of Environmental Sciences, University of California, Riverside, CA 92521, USA
[e] Agrosphere (IBG-3), Institute of Bio- and Geosciences, Forschungszentrum Jülich GmbH, Jülich, Germany

ARTICLE INFO

Article history:
Received 26 March 2019
Received in revised form
28 June 2019
Accepted 26 August 2019
Available online 28 August 2019

Keywords:
Calcium carbonate
Engineered silver nanoparticles
Stabilizing agent
Blocking
Soil organic matter

ABSTRACT

The transport and retention behavior of polymer- (PVP-AgNP) and surfactant-stabilized (AgPURE) silver nanoparticles in carbonate-dominated saturated and unconsolidated porous media was studied at the laboratory scale. Initial column experiments were conducted to investigate the influence of chemical heterogeneity (CH) and nano-scale surface roughness (NR) arising from mixtures of clean, positively charged calcium carbonate sand (CCS), and negatively charged quartz sands. Additional column experiments were performed to elucidate the impact of CH and NR arising from the presence and absence of soil organic matter (SOM) on a natural carbonate-dominated aquifer material. The role of the nanoparticle capping agent was examined under all conditions tested in the column experiments. Nanoparticle transport was well described using a numerical model that facilitated blocking on one or two retention sites. Results demonstrate that an increase in CCS content in the artificially mixed porous medium leads to delayed breakthrough of the AgNPs, although AgPURE was much less affected by the CCS content than PVP-AgNPs. Interestingly, only a small portion of the solid surface area contributed to AgNP retention, even on positively charged CCS, due to the presence of NR which weakened the adhesive interaction. The presence of SOM enhanced the retention of AgPURE on the natural carbonate-dominated aquifer material, which can be a result of hydrophobic or hydrophilic interactions or due to cation bridging. Surprisingly, SOM had no significant impact on PVP-AgNP retention, which suggests that a reduction in electrostatic repulsion due to the presence of SOM outweighs the relative importance of other binding mechanisms. Our findings are important for future studies related to AgNP transport in shallow unconsolidated calcareous and siliceous sands.

1. Introduction

Engineered silver nanoparticles (AgNPs) are frequently applied in textiles and personal care products due to their antimicrobial and antifungal properties (Maillard and Hartemann, 2013; Panacek et al., 2009). Their release into the environment (Farkas et al., 2011; Kaegi et al., 2010), bioavailability (Navarro et al., 2008) and potentially toxic or detrimental effects on a multitude of organisms (Juganson et al., 2017; Makama et al., 2016; Mallevre et al., 2014; Siller et al., 2013) have been well documented in the scientific literature. Recent studies have demonstrated and discussed their occurrence in surface waters (Peters et al., 2018), wastewater treatment plant influents/effluents (Kaegi et al., 2013; Kaegi et al., 2011) and sewage sludge (Bäuerlein et al., 2017).

Transport studies for AgNPs have been carried out to improve our understanding of factors that control their environmental fate and to better assess potential risks. Many previous transport

☆ This paper has been recommended for acceptance by Baoshan Xing.

* Corresponding author. USDA-ARS, U.S. Salinity Laboratory, 450 W. Big Springs Road, Riverside, CA, 92507, USA.
E-mail address: scott.bradford@ars.usda.gov (S.A. Bradford).

https://doi.org/10.1016/j.envpol.2019.113124
0269-7491/

studies have been conducted in pure quartz sands (Liang et al., 2013b; Tian et al., 2010), topsoils (Braun et al., 2015; Cornelis et al., 2013; Liang et al., 2013a; Makselon et al., 2018; Makselon et al., 2017; Sagee et al., 2012), sand filters (Degenkolb et al., 2018), or consolidated rock such as sandstone (Neukum et al., 2014a,b). Calcium-based carbonate minerals such as calcite ($CaCO_3$) or dolomite ($CaMg[CO_3]_2$) are major components of carbonate aquifers around the world that are vital for drinking-water production (Bayat et al., 2014). However, only few studies on engineered nanoparticle transport through carbonate-dominated material exist. Rahmatpour et al. (2018) compared polyvinylpyrrolidone (PVP)-coated AgNP transport through pure quartz sand and two calcareous topsoils with considerable clay content (sandy loam and loam). They found that their two topsoils retained around 99% of the injected PVP-AgNPs, whereas pure quartz sand retained about 11%. Experiments with graphene oxide nanoparticles in limestone porous media show an increase in mobility associated with increasing pH and humic acid concentration (Dong et al., 2017). Bayat et al. (2014) and Bayat et al. (2015) studied the transport of Al_2O_3 and TiO_2 nanoparticles through limestone by varying the background solution. Laumann et al. (2013) showed that the mobility of polydisperse nano zero-valent iron strongly decreases with increasing carbonate content in crushed limestone. These authors attributed retention of negatively charged nanoparticles in limestone to cation bridging and elimination of the energy barrier to attachment by charge heterogeneity and/or near neutral zeta potentials (Laumann et al., 2013; Dong et al., 2017; Rahmatpour et al., 2018), as well as to the morphology of the limestone (Bayat et al., 2014, 2015). Systematic studies considering predefined unconsolidated mixtures of carbonate- and quartz-based sands as well as natural carbonate-rich aquifer material do not exist in the literature to the knowledge of the authors.

The charge of calcite surfaces is determined by the presence of Ca^{2+} and CO_3^{2-} in the diffuse layer (Al Mahrouqi et al., 2017; Heberling et al., 2011). The zero point of charge for pure calcite is around 8 to 9.5 (Somasundaran and Agar, 1967), so it is expected to possess a net positive charge under neutral pH conditions. However, a negative surface charge on calcite may arise from impurities with lower zero points of charge such as silicate minerals (Chen et al., 2014) or when soil organic matter (SOM) is adsorbed onto its surface (Al Mahrouqi et al., 2017; Vdović, 2001), and thus, charge heterogeneity on the calcite surfaces is expected.

Soil (or sediment) charge heterogeneity has frequently been reported to strongly influence nanoparticle transport and retention by locally reducing or eliminating the energy barrier for primary minimum interactions (Bendersky and Davis, 2011; Bradford et al., 2017). However, no research has systematically examined the influence of calcite with impurities from silicate minerals and/or SOM coatings on AgNP transport. Chemical heterogeneities (CH) in such media will produce variations in charge, Hamaker constant (Bradford et al., 2018), and/or hydrophobicity (Tschapek, 1984).

Humic acid (HA), an amphiphilic component of SOM, has been found to stabilize and enhance the transport of AgNPs (Park et al., 2016; Yang et al., 2014), as well as other nanoparticles (Wang et al., 2012), in porous media. Enhanced nanoparticle transport in the presence of HA, surfactants, and SOM has been attributed to decreases in the electrostatic attraction, increases in steric repulsion, and competitive blocking of retention sites (Ryan et al., 1999). However, the stabilizing effect of SOM has been found less distinct for PVP-coated AgNP compared to citrate-coated AgNP due to differences in the bonding energy between the capping agent and the silver, which is higher in the case of PVP (Gunsolus et al., 2015). Consequently, interactions of SOM with AgNPs are expected to depend on the physicochemical properties of the SOM and the AgNP capping agent, although limited research has examined this specific issue to date.

Differences in soil mineral weathering (e.g., quartz and calcite) and SOM coatings are anticipated to influence the nanoscale roughness (NR) properties of porous media. Furthermore, the conformation of SOM coatings can change depending on the water content as well as the solution chemistry (Sposito, 2008). Various capping agents may also alter the roughness properties of AgNPs. The collector surface roughness has been found to play an important role in controlling the mobility and fate of nanoparticles due to its strong influence on interaction energies, hydrodynamic forces, and lever arms associated with hydrodynamic and adhesive torques (Morales et al., 2009; Torkzaban et al., 2010). When small amounts of NR occur on both porous medium and colloid surfaces the magnitudes of the secondary and primary minima, and the energy barriers are all strongly reduced in comparison to a smooth surface (Bendersky and Davis, 2011; Bhattacharjee et al., 1998; Bradford et al., 2018; Bradford and Torkzaban, 2013; Hoek and Agarwal, 2006), and the colloid may be susceptible to diffusive and/or hydrodynamic removal (Bradford and Torkzaban, 2015; Rasmuson et al., 2017). These changes in the interaction energy profile may even occur in the presence of CH, such that electrostatically favorable locations are unfavorable for colloid retention (Zhang et al., 2016). However, the coupled influence of CH and NR from calcite minerals, SOM, and capping agents has not yet been studied.

Here we conduct laboratory-scale column experiments and numerical modeling to systematically study the transport and retention behavior of polymer- and surfactant-stabilized AgNPs in carbonate-dominated saturated and unconsolidated porous media. Our research provides novel experimental data that provide new insight into AgNP mobility related to the influence of soil/sediment CH and NR. First, we examine the influence of CH and NR arising from mixtures of clean calcium carbonate and quartz sands. Next, we study the influence of CH and NR arising from the presence and absence of SOM on a natural carbonate-dominated aquifer material. Finally, the role of the AgNP capping agent is inspected under both of these soil CH and NR conditions. These results are interpreted using mathematical modeling of AgNP transport and blocking behavior on one or two kinetic retention sites, calculations to determine the fraction of the porous media surface that contributed to retention, and interaction energy calculations that considered the influence of various fractions of nanoscale roughness.

2. Material and methods

2.1. Silver nanoparticles and electrolyte solution

For the laboratory experiments, we used two commercially available types of AgNPs. The first type was sterically stabilized silver nanoparticles AgPURE™ W-10 (ras materials, Regensburg, Germany) from a stock suspension with an AgNP concentration of 10.16% (weight per weight, w/w) and identical to the OECD reference material NM300K. According to Klein et al. (2011), AgPURE™ stabilization is achieved using 4% w/w of polyoxyethylene glycerol trioleate and 4% w/w of polyoxyethylene (20) sorbitan monolaurate (Tween 20). Additionally, AgPURE™ W-10 contains 7.5% (w/w) ammonium nitrate (Menzel et al., 2013). About 99% of the spherically-shaped particles are in a size range of 15–20 nm. Their hydrodynamic diameter was found to be stable over 24 h in 1 mM KNO_3 at 45.1 ± 4.5 nm (Liang et al., 2013b), in 1 mM Na^+ at 51.0 ± 1.3 nm and in 1 mM Ca^{2+} at 56.4 ± 1.5 nm (Adrian et al., 2018). The original suspension also contains 5% of free/unbound surfactant and less than 1% of the total silver mass was released as

Ag^+ within three days (Liang et al., 2013b).

The second type of AgNP used in this work was coated with PVP (Getnanomaterials GNM, OOCAP SAS, France, stock number: 7023HZ, powder form). Data provided by the manufacturer shows that the PVP-AgNP powder consists of 10% silver (purity of 99.99%), 89.8% PVP and 0.2% moisture. The PVP-AgNP diameter is 20 nm and the density 2.07 g cm^{-3}. Adrian et al. (2018) showed that the PVP-AgNP is stable in 1 mM Na^+ and 0.1 mM Ca^{2+} with hydrodynamic diameters of 66.9 ± 4.4 nm and 61.8 ± 0.9 nm, respectively.

Electrolyte solutions were prepared using ultrapure water (Merck Millipore Milli-Q, 18.2 MΩ cm, TOC: 1–2 ppb, 0.22 μm membrane filter) and 1 mM $NaHCO_3$ (Merck KGaA, Darmstadt, Germany) with a pH of 8.3. To better compare our results with other studies using column experiments (Liang et al., 2013a; Wang et al., 2014), the total silver concentration in the influent solution (C_0) for transport experiments was adjusted to 10 mg L^{-1}, which is above reported concentrations found in soil, surface or groundwater (Klitzke et al., 2015; Peters et al., 2018; Troester et al., 2016; Yecheskel et al., 2018).

Transmission electron microscopy (TEM) was performed to provide further information on the size and shape of the AgNPs. Samples were dispersed in an ultra-sonic bath for 15 min. Copper specimen grids coated with an ultrathin layer of carbon (Plano GmbH, Germany) were immersed in the sample solution and then air-dried. Micrographs were obtained using a CM 20 FEG (Philips, Netherlands) operating at 200 keV.

2.2. Porous media

To study the effect of varying calcium carbonate sand (CCS) content on AgNP transport, five mixtures of natural quartz sand (Schlingmeier Quarzsand GmbH & Co. KG, Schwülper, Germany) and CCS were prepared, with CCS contents (w/w) of 0, 20, 50, 80 and 100%, respectively. According to the distributors, the natural quartz sand (average particle density of 2.65 g cm^{-3}) consisted of 99.5% SiO_2, 0.02% K_2O, 0.036% Fe_2O_3, 0.01% TiO_2, and other minor fractions, while the CCS (average particle density of 2.70 g cm^{-3}, Ulmer Weiss from Eduard Merkle GmbH & Co. KG, Blaubeuren, Germany) contained 99.2% (weight) $CaCO_3$, 0.4% $MgCO_3$, about 0.135% iron oxides and aluminum oxides, and 0.25% SiO_2. Both materials were wet sieved into size fractions of 0.71–1 mm and 1–1.25 mm, and then cleaned to remove organic impurities using the methods of Chu et al. (2001) for the quartz sand (i.e. soaked in 30% H_2O_2 for 24 h) and Mikutta et al. (2005) for the CCS (described below). The sand was subsequently oven dried before use. Each column experiment employed a selected CCS content with a similar grain size distribution. The median grain size diameter for CCS mixtures was determined to be 0.92 mm with a coefficient of uniformity of 1.3 and coefficient of curvature of 0.9.

The natural carbonate-dominated aquifer material was obtained from an open pit mine near Eching, Germany (Münchner Kiesunion GmbH & Co. Sand-und Kieswerke KG, Unterschleißheim, Germany). It was sieved following DIN 18123 (2011) to obtain a size range from 0.063 to 2 mm and a median grain diameter (d_{50}) of 0.7 mm. The average particle density was determined according to DIN 18124 (2011) using pycnometers (n = 3). The mineralogy of the aquifer material was determined by means of X-ray powder diffraction (XRD) using a Siemens D5000. To evaluate the effect of SOM on natural aquifer material, experiments with cleaned and uncleaned material were conducted. Cleaning of the material was performed using the method suggested by Mikutta et al. (2005). In brief, SOM from the grain surfaces was removed by soaking each grain size fraction three times over 24 h in NaClO (Hedinger, Stuttgart, Germany) that was diluted to 6%, adjusted to pH = 8.5, and at room temperature. Note that this NaClO solution causes no dissolution of mineral components (Gaffey and Bronnimann, 1993). Therefore it is expected that roundness and sphericity of the porous medium will not significantly change. After three cleaning cycles, the material was rinsed with ultra-pure water over a 21 μm PES membrane (Franz Eckert GmbH, Waldkirch, Germany) and oven-dried at 50 °C. The organic matter content was determined by weight loss. The pH of all porous media used was determined according to DIN EN 15933 (2012) in 10 mM $CaCl_2$ in the absence and presence of SOM.

A CamSizer P4 (Retsch Technology, Germany) was employed to determine roundness and sphericity of the CCS, quartz sand, and the aquifer material (cleaned and uncleaned), respectively. The surface area of all materials was determined by N_2-BET measurements (n = 3). The zeta potential of all materials was measured using a Malvern ZetaSizer Nano ZS (Malvern GmbH) by the method presented in Sondi et al. (2009). In short, the respective material mixtures were crushed, and 40 mg of each was dispersed in 100 mL of the background solution at 25 °C before measurements.

2.3. Transport experiments

Transport experiments were carried out in borosilicate glass columns with an inner diameter of 2.6 cm, a length of 15 cm, and a volume of 79.6 mL. The columns were wet-packed in 1 mM $NaHCO_3$. The porosity of the material packed into each column is provided in Table 2. A 2 mm-layer of quartz wool was used at the column inlet and outlet to retain fine particles in the material matrix. All experiments were conducted in an up-flow mode using a peristaltic pump (ICP High Precision Multichannel Dispenser, Ismatec). The average pore water velocity in the experiments was 8.64 m d^{-1}. Before AgNP transport experiments, tracer tests with NaBr (Merck KGaA, Darmstadt, Germany) were run. For that, the columns were first flushed with at least 20 pore volumes (PV) of 1 mM $NaHCO_3$. Each tracer test consisted of flushing 3 PV of NaBr in 1 mM $NaHCO_3$ solution through the column, followed by continued elution with 3 PV of 1 mM $NaHCO_3$ to prevent dissolution of the carbonate material. After each tracer test, the respective column was again flushed with 20 PV of 1 mM $NaHCO_3$ before at least 3 PV of AgNP suspension was injected, followed again by flushing with at least 3 PV of AgNP-free 1 mM $NaHCO_3$. Column effluent fractions

Table 1
Zeta potential (n = 3) of the porous media and silver nanoparticles in 1 mM $NaHCO_3$ at pH = 8.3 and temperature of 25 °C, hydrodynamic diameter (d_H, n = 6) of PVP-coated AgNP and AgPURE in 1 mM $NaHCO_3$ at pH = 8.3, roundness and sphericity information obtained from CamSizer measurements and BET surface area of the porous medium.

Sample	Zeta potential	d_H	Roundness	Sphericity	BET
	[mV]	[nm]	[-]	[-]	[m^2 g^{-1}]
Quartz sand	−60.7		0.65	0.75	0.13
CCS	+1.1		0.33	0.64	0.21
Eching (uncleaned)	−26.1		0.44	0.72	1.09
Eching (cleaned)	−30.0				0.94
PVP-AgNP	−9.8	60.9 ± 1.1			
AgPURE	−17.1	51.1 ± 0.2			

Table 2
Summary of experimental conditions and simulated parameter values of surfactant- and polymer-stabilized AgNP in calcium carbonate sand and carbonate-dominated aquifer material.

Fig.	AgNP	φ	d_{50}	CCS	Q	λ_L	S_{max1}/C_0	k_{sw1}	S_{max2}/C_0	k_{sw2}	R^2	AgNP input	M_{eff}	M_{solid}	M_{total}	SOM	S_f
		[-]	[mm]	[%]	[m s^{-1}] × 10^{-5}	[m] × 10^{-2}	[cm^3 g^{-1}]	[s^{-1}] × 10^{-4}	[cm^3 g^{-1}]	[s^{-1}] × 10^{-4}	[-]	[mL]	[%]	[%]	[%]		[-] × 10^{-4}
2a	AgPURE	0.38	0.9	0	2.9	0.39	–	0.98	–	–	0.98	90.12	81.10	9.20	90.30	No	–
S1a	AgPURE	0.38	0.9	20	4.0	0.32	0.17	3.66	–	–	0.95	108.578	75.31	4.07	79.37	No	16.63
2a	AgPURE	0.38	0.9	50	4.1	0.28	0.14	6.11	–	–	0.93	97.84	84.46	4.67	89.13	No	11.64
S1a	AgPURE	0.44	0.9	80	3.6	0.29	0.38	2.42	–	–	0.98	114.58	76.09	25.17	101.26	No	27.47
2a	AgPURE	0.46	0.9	100	3.8	0.78	0.29	14.50	–	1.17	0.95	193.60	70.9	23.41	94.31	No	19.29
2b	PVP-AgNP	0.37	0.9	0	3.8	0.19	0.10	5.38	–	–	0.98	90.01	85.82	10.5	96.32	No	39.27
S1b	PVP-AgNP	0.41	0.9	20	4.2	0.38	0.05	151.00	–	1.55	0.99	134.60	76.88	23.07	99.95	No	17.32
2b	PVP-AgNP	0.43	0.9	50	4.4	0.19	0.42	6.36	–	–	0.97	122.56	69.00	21.00	90.00	No	123.69
S1b	PVP-AgNP	0.44	0.9	80	4.5	0.18	1.25	36.00	–	–	0.85	214.57	32.40	61.83	94.23	No	320.11
2b	PVP-AgNP	0.45	0.9	100	4.4	0.29	1.49	28.90	–	–	0.96	237.35	28.36	72.63	100.99	No	351.04
3a	AgPURE	0.39	0.7	Eching	3.8	0.41	0.12	8.05	–	–	0.95	181.18	87.40	12.1	99.50	No	1.70
3a	AgPURE	0.39	0.7	Eching	3.9	0.86	0.06	18.80	0.52	5.29	0.96	186.53	64.90	10.98	75.87	Yes	7.08
3b	PVP-AgNP	0.39	0.7	Eching	4.0	1.15	0.35	92.80	0.40	6.13	0.99	189.59	51.50	14.83	66.33	No	37.60
3b	PVP-AgNP	0.39	0.7	Eching	4.0	0.56	0.24	125.00	0.48	8.44	0.99	189.30	52.58	27.33	79.91	Yes	31.12

φ: porosity, determined gravimetrically; d_{50}: mean grain size diameter; CCS: Calcium carbonate sand content in the artificially mixed porous media; q: Darcy velocity (discharge per unit area); λ_L: dispersivity obtained from tracer experiments; S_{max1}: maximum solid phase concentration on the first sorption site; k_{sw1}: first-order retention coefficient for the first sorption site; S_{max2}: maximum solid phase concentration on the second sorption site; k_{sw2}: first-order retention coefficient for the second sorption site; R^2: coefficient of determination; AgNP input: volume of AgNP suspension injected into the column; M_{eff}: mass recovery in the effluent; M_{solid}: mass recovery in the soil; M_{total}: total mass recovery; SOM: soil organic matter; *Sf*: solid surface area available for retention.

were collected in polypropylene centrifuge tubes (VWR International GmbH. Germany) using a fraction collector (Pharmacia FRAC-100 Fraction Collector, Amersham Biosciences). For each pore volume three to four samples were analyzed. Inflow and outflow pH were monitored using a SenTix 41 pH electrode (WTW, Weilheim, Germany).

The total Ag concentration in effluent samples was determined using ICP-MS (Agilent 7900 ICP-MS, Agilent Technologies). The electrophoretic mobility of the AgNPs in the stock solution (n = 3 for each background solution) was determined with a Malvern Zetasizer Nano ZS at 25 °C and then converted to a zeta potential [mV] using the Smoluchowski equation.

At the end of the transport experiments, the column material of selected experiments was carefully extracted in 1 cm layers, oven dried, and homogenized to generate retention profiles. For this, 0.5 g of the homogenized porous medium was transferred into a 50 mL centrifuge tube and acidified using 5 mL HNO_3 (w/w 65%). The total silver concentration was determined using ICP-MS. Most AgNP transport experiments were replicated, and results are shown in the supporting information (SI).

Section S1 of the SI provides detailed information about modeling the tracer and AgNP transport experiments, which was done with the numerical finite element code HYDRUS 1D (Šimůnek et al., 2008; Šimůnek et al., 2016). For the AgNP experiments, Langmuirian blocking with two kinetic retention sites was assumed. Inversely determined model parameters included the retention rate coefficients (k_{sw1} and k_{sw2}) and the maximum solid phase AgNP concentrations (S_{max1} and S_{max2}), where the subscripts 1 and 2 on parameters denote the site. Fitted values of S_{max1} and S_{max2} were used to determine the fraction of the solid surface area that contributed to AgNP retention (S_f) using Eq. (S5). The Akaike information criterion (AIC) (Akaike, 1974) was calculated to quantitatively compare the quality of different models for AgNP retention. It was applied to justify the use of one or two retention sites in the various models.

Interaction energy calculations that considered various surface roughness fractions ($f_{rs} = 0$, 0.01, 0.025, 0.05, and 0.1) and a roughness height (h_{rs}) of 35 nm were performed to better understand mechanisms contributing to AgNP retention on the various sands (quartz, carbonate, the Eching aquifer material (denoted below as Eching), and Eching without SOM) in 1 mM $NaHCO_3$ at pH = 8.3 solution. Section S2 of the SI provides details about these calculations for AgNP-sand interactions. The dimensionless depths of the primary (Φ_{1min}) and secondary (Φ_{2min}) minima, and the energy barrier height (Φ_{max}) were obtained by analyzing the interaction energy profiles.

3. Results and discussion

3.1. Characterization of AgNPs and porous media

TEM images (Fig. 1) show the near-spherical nature of the AgNPs with diameters of around 16–20 nm for AgPURE and 11–25 nm for PVP-AgNP, respectively. Hydrodynamic diameters (d_H) were found to be around 51.1 nm ± 0.2 nm for AgPURE and 60.9 nm ± 1.1 nm for PVP-AgNP in influent samples determined via DLS (Table 1), which is in good agreement with previous studies (Liang et al., 2013b; Adrian et al., 2018). The zeta potential was slightly more negative for AgPURE (−17.1 mV) than PVP-AgNP (−9.8 mV) in 1 mM $NaHCO_3$, which suggests a potential for greater suspension stability.

CamSizer measurements (Table 1, on a scale from 0 to 1) revealed that the quartz sand had the highest roundness (0.65) and sphericity (0.75), while the CCS was less rounded (0.33) and less spherical (0.64). The total organic carbon content of the quartz sand

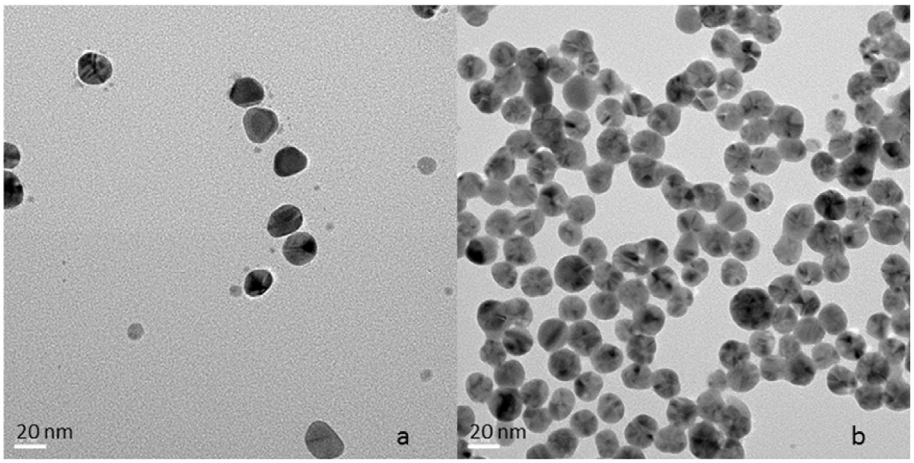

Fig. 1. TEM images of a) PVP-AgNPs and b) AgPURE at 20 nm range.

following H_2O_2 treatment was determined by ignition loss as 0.091%. The BET measurements showed a higher surface area for the CCS (0.21 $m^2\,g^{-1}$) as compared to the quartz sand (0.13 $m^2\,g^{-1}$). This implies that the CCS had more roughness and/or internal porosity than the quartz sand. At pH 8.3, the zeta potential of the quartz sand was more negative (−60.7 mV) compared to the AgNPs (Table 1). In contrast, the CCS showed a slightly positive zeta potential (+1.1 mV). A positive zeta potential was also encountered by Vdović (2001) for synthetic calcium carbonate at pH = 8.4 ± 0.1 in the absence of organic matter. The AgNPs are therefore expected to exhibit electrostatic attraction for the CCS and repulsion for the quartz sand, especially for AgPURE.

Results from the X-ray diffraction analysis (Table S1) showed that the natural aquifer (Eching) material was dominated by carbonate minerals (56.1% calcite and dolomite), while 37.6% are quartz minerals. Chlorite clay minerals, smectite clay minerals, and kaolinite are present only in small amounts (<1.4%). The rest of the material is formed by microcline and albite. The average particle density for the Eching material was determined from pycnometer experiments to be 2.733 g cm^{-3}, which is close to that of pure calcite with 2.7 g cm^{-3}. The uncleaned Eching material had a BET surface area of 1.09 $m^2\,g^{-1}$, whereas the surface area decreased to 0.94 $m^2\,g^{-1}$ (Table 1) after the removal of SOM, which also produced a weight loss of 0.24 ± 0.07% on the natural carbonate-dominated material. SOM consists of a complex mixture of fulvic acid, humic acid, and humin fractions (Huang et al., 2003) that includes carboxylic and phenolic groups (MacCarthy and Rice, 1985), biopolymers such as lignin and polysaccharides (MacCarthy and Rice, 1985), mineral-bound lipids and humic acid-like materials (Rice and MacCarthy, 1990), and kerogen and black carbon (Song et al., 2002). The presence of calcium carbonate in a porous medium can be accompanied by free excess Ca^{2+} which can inhibit the degradation of SOM by forming Ca-SOM bridges (Clough and Skjemstad, 2000). Although the SOM fraction of the Eching soil is very small, it can coat large portions of the exposed mineral surface (Doerr et al., 2000). DLS measurements show that the Eching material exhibited a negative zeta potential in the presence of SOM (−26.1 mV) due to a fairly large fraction of quartz minerals (Table 1). After cleaning, the zeta potential further decreased to −30.0 mV. Consequently, a net repulsive electrostatic interaction is expected between the AgNPs and the Eching aquifer material with and without SOM.

The pH of the artificial quartz-carbonate sand mixtures in 10 mM $CaCl_2$ increased with increasing CCS content from 5.8 (100% quartz sand) to 8.4 (100% CCS). During the transport experiments, the pH of the influent remained stable at 8.3 ± 0.1 in 1 mM $NaHCO_3$. For experiments with pure quartz sand, the effluent pH remained at 8.3 ± 0.1 while the effluent pH in experiments with CCS only slightly increased to 8.4 ± 0.1. This small increase in the effluent pH can be attributed to the buffering capacity of calcium carbonate (Dong et al., 2017). The pH of the natural aquifer material was determined at 8.4 ± 0.1 (n = 3) before and 8.5 ± 0.1 (n = 3) after cleaning of SOM. Here, the effluent pH was 8.4 ± 0.1.

Dissolution of calcium carbonate during our transport experiments and its effect on the AgNPs was considered negligible for two reasons. First, Ca^{2+} concentrations in selected effluent samples were never higher than 0.01 mM in our experiments, as determined by ICP-MS (data not shown). This concentration is much lower than the 2.5 mM, for which Topuz et al. (2014) and Topuz et al. (2015) did not observe any significant effect on the agglomeration behavior of PVP-AgNPs. Second, Topuz et al. (2014) demonstrated that prolonged exposure of PVP-AgNPs to carbonate (over a week) had little effect on agglomeration behavior. Our experiments did not take longer than 4.5 h, and the hydrodynamic diameters of AgNPs in the presence of calcium carbonate did not significantly change during this time interval.

3.2. *Effect of calcium carbonate content and stabilizing agent on AgNP transport*

Fig. 2a and b present observed and simulated breakthrough curves (BTCs) for AgPURE (Fig. 2a) and PVP-AgNPs (Fig. 2b) in porous media containing 0, 50 and 100% CCS content. Figs. S1a and S1b also contain information on 20 and 80% mass of CCS. Retention profiles (RPs) for 0% and 100% CCS are presented in the SI (Fig. S2). Fig. 2a and b also show example BTCs for the conservative bromide tracer. All tracer tests showed nearly complete recovery of bromide (97.6–102.6%) and breakthrough close to 1 PV. The bromide tracer breakthrough occurs in almost all cases before AgNP breakthrough, which indicates that pore-size exclusion of AgNPs was not significant. Table 2 provides a summary of the considered physicochemical conditions, measured and fitted model parameters, and mass balance information for all AgNP transport experiments. The total mass recovery of AgNPs in the experiments shown in Table 2 varied between 79.4 and 101.3%. Standard errors and confidence intervals of the fitted parameters as well as values of the AIC are provided in the SI (Tables S2 and S3). Replicate experiments conducted for the CSS/quartz sand mixtures are listed in Table S2. In

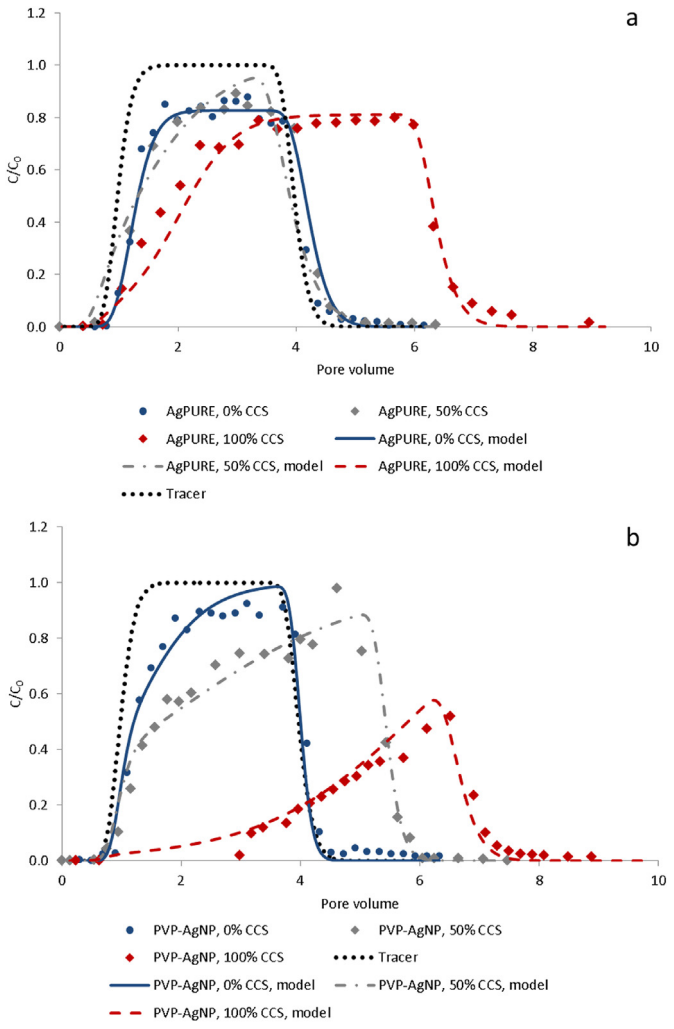

Fig. 2. Breakthrough curves of AgPURE (a) and PVP-AgNP (b) transport experiments in quartz sand and calcium carbonate sand (CCS) with various mass percentages of CCS in the artificially mixed porous medium. Pore water velocity = 8.64 m d^{-1} and d_{50} = 0.9 m.

general, replicate experiments agreed well with the results of the experiments shown in Table 2 as can be assessed by comparison of fitted model parameters and effluent mass balance information for AgNPs that are presented in Table S3.

AgPURE was highly mobile in the various CCS mixtures, with the effluent mass ranging from 70.9 to 84.5% (Table 2). Breakthrough of AgPURE (Fig. 2a and S1a) occurred at around 1 PV, rapidly increased and reached a plateau, and exhibited little blocking behavior when CCS $\leq$ 80%. Conversely, the breakthrough of AgPURE in pure CCS (100% $CaCO_3$) was retarded, and then slowly increased to a similar plateau as the other CCS mixtures. The RPs for AgPURE (Fig. S2a) showed nearly uniform distribution with depth.

The effluent mass of PVP-AgNP rapidly and systematically decreased with increasing CCS percentage from 85.8% to 28.4% (Table 2). This reflects an increase in the amount of PVP-AgNP retention with the CCS percentage. The PVP-AgNP BTCs clearly showed blocking behavior when CCS $\geq$50% (Fig. 2b and S1b) and exhibited greater delay in breakthrough with increasing CCS percentage. Decreasing breakthrough with increasing carbonate content (however no significant retardation) was similarly observed by Laumann et al. (2013) for PAA-nZVI nanoparticles in crushed limestone. At CCS above 20%, much greater retention of PVP-AgNP occurred than of AgPURE (comparison of Figs. S1a and S1b). However, both PVP-AgNP and AgPURE exhibit an increased delay in breakthrough and blocking behavior with increasing CCS percentages.

The shape of the PVP-AgNP RP in pure quartz sand was uniform, whereas in 100% CCS the RP shape was nonmonotonic (Fig. S2b). Other researchers have observed nonmonotonic RPs for AgNPs and other nanoparticles (e.g. Liang et al., 2013b) and have attributed their findings to a number of factors, including: competitive blocking from free surfactants and/or polymers (Becker et al., 2015; Liang et al., 2013b), solid phase migration (Bradford et al., 2011; Johnson et al., 2018), and reversible blocking (Leij et al., 2015). All of these factors may contribute to the development of nonmonotonic RPs in our experiments, but the relative importance of these factors cannot be deduced from the collected information and is beyond the scope of the present study.

Observed BTCs in Fig. 2a and b were reasonably well described using the mathematical model outlined in the SI, with coefficients of determination (R^2) ranging from 0.85 to 0.99. The AIC values indicated that blocking was not needed to describe the BTC for AgPURE in pure quartz sand, otherwise blocking was always justified on site 1 (see Table S2 in the SI for AIC values). A second retention site was sometimes needed to describe the BTC data (e.g., CCS = 100% for AgPURE and CCS = 20% for the PVP-AgNPs, see e.g. Fig. S4), but the AIC indicated that blocking was not warranted on this site. Collectively, the modeling results indicate that blocking played an important role in AgNP fate. Other researchers have similarly reported the importance of blocking on colloid and nanoparticle transport through porous media (Adrian et al., 2018; Liang et al., 2013a; Wang et al., 2015), and noted the need to consider two retention sites (Bradford et al., 2014; Sasidharan et al., 2014). The mathematical model did not provide a good description of the nonmonotonic PVP-AgNPs RPs. Simulation of nonmonotonic RPs requires the use of more complex mathematical formulations which increase the uncertainty in parameter estimates (e.g., Bradford et al., 2011; Johnson et al., 2018), and was beyond the scope of the current study.

Table 2 indicates that k_{sw1} and S_{max1} tended to increase with the CCS percentage. This trend is expected because attachment is electrostatically favorable and rapid between negatively charged AgNPs and the slightly positively charged calcium carbonate material (Table 1). Values of k_{sw1} and S_{max1} are generally greater for PVP-AgNPs than AgPURE at a given CCS percentage. This behavior cannot be explained by electrostatic considerations which predict a greater electrostatic attraction between the calcium carbonate and the more negatively charged AgPURE than the PVP-AgNPs (Tables 1 and 3). Furthermore, the values of S_f that were determined from fitted values of S_{max1} using Eq. (S5) from the SI were very small (e.g., <0.04 in Table 2). This indicates that only a small fraction of the surface contributed to AgNP retention, even under the best-case scenario of positive electrostatic interactions (e.g., carbonate in Table 3, CCS = 100% and AgPURE). Consequently, consideration of chemical heterogeneity alone cannot explain the observed AgNP retention behavior. Potential explanations for these deviations will be considered below.

The presence of surfactants and/or polymers on the surface of AgNPs has been reported to decrease colloid retention due to steric repulsion (Yang et al., 2014). Steric repulsion is predicted to produce a large energy barrier to attachment that should hinder any AgNP retention on the collector surface (Israelachvili, 2011). This result is clearly not consistent with the experimental observations shown in Figs. 2 and 3. An alternative explanation of the observed AgNP retention behavior is due to nanoscale roughness which is ubiquitous on natural surfaces (Suresh and Walz, 1996) and AgNPs due

Table 3
The predicted dimensionless energy barrier (Φ_{max}) and primary minima (Φ_{1min}) for AgPURE and PVP-AgNPs with the various sands in 1 mM $NaHCO_3$ solution at pH = 8.3 when the sand roughness height (h_{rs}) is 35 nm and the roughness fraction (f_{rs}) is varied from 0 to 0.1.

AgNP	Sand	f_{rs} [-]	h_{rs} [nm]	Φ_{max} [-]	Φ_{1min} [-]
AgPURE	Quartz	0	35	15.3	−72.8
AgPURE	Quartz	0.01	35	1.2	0.7
AgPURE	Quartz	0.025	35	1.3	−0.4
AgPURE	Quartz	0.05	35	1.6	−2.3
AgPURE	Quartz	0.1	35	2.3	−6.0
AgPURE	CCS	0	35	0.0	−29.4
AgPURE	CCS	0.01	35	0.0	−0.3
AgPURE	CCS	0.025	35	0.0	−0.8
AgPURE	CCS	0.05	35	0.0	−1.5
AgPURE	CCS	0.1	35	0.0	−3.0
AgPURE	Eching	0	35	12.3	1.2
AgPURE	Eching	0.01	35	0.7	0.6
AgPURE	Eching	0.025	35	0.8	0.6
AgPURE	Eching	0.05	35	1.1	0.6
AgPURE	Eching	0.1	35	1.7	0.7
AgPURE	Eching w/o SOM	0	35	13.2	−0.7
AgPURE	Eching w/o SOM	0.01	35	0.8	0.7
AgPURE	Eching w/o SOM	0.025	35	0.9	0.7
AgPURE	Eching w/o SOM	0.05	35	1.2	0.6
AgPURE	Eching w/o SOM	0.1	35	1.8	0.6
PVP-AgNP	Quartz	0	35	6.0	−148.9
PVP-AgNP	Quartz	0.01	35	0.6	−0.6
PVP-AgNP	Quartz	0.025	35	0.6	−2.8
PVP-AgNP	Quartz	0.05	35	0.6	−6.6
PVP-AgNP	Quartz	0.1	35	0.9	−14.0
PVP-AgNP	CCS	0	35	0.0	−21.1
PVP-AgNP	CCS	0.01	35	0.0	−0.2
PVP-AgNP	CCS	0.025	35	0.0	−0.6
PVP-AgNP	CCS	0.05	35	0.0	−1.1
PVP-AgNP	CCS	0.1	35	0.0	−2.1
PVP-AgNP	Eching	0	35	5.5	−18.5
PVP-AgNP	Eching	0.01	35	0.4	0.2
PVP-AgNP	Eching	0.025	35	0.4	−0.1
PVP-AgNP	Eching	0.05	35	0.5	−0.5
PVP-AgNP	Eching	0.1	35	0.8	−1.5
PVP-AgNP	Eching w/o SOM	0	35	5.7	−25.7
PVP-AgNP	Eching w/o SOM	0.01	35	0.4	0.2
PVP-AgNP	Eching w/o SOM	0.025	35	0.5	−0.2
PVP-AgNP	Eching w/o SOM	0.05	35	0.6	−0.8
PVP-AgNP	Eching w/o SOM	0.1	35	0.8	−2.1

CCS: calcium carbonate sand; SOM: soil organic matter.

to adsorbed surfactants and/or polymers. Table 3 provides calculated interaction energy parameters for AgPURE and PVP-AgNPs on the various sands when $h_{rs} = 35$ nm and $f_{rs} = 0$, 0.01, 0.025, 0.05, and 0.1. Consistent with these results, NR pillars are predicted to locally reduce or eliminate the energy barrier (Bhattacharjee et al., 1998; Hoek and Agarwal, 2006), and decrease the magnitudes of the primary and secondary minima (Bradford et al., 2017; Torkzaban and Bradford, 2016). These effects on the interaction energy profile are most pronounced when small fractions of NR pillars occur on both the surfaces of the colloid and collector (Bradford et al., 2017), and produce conditions that are susceptible to diffusive or hydrodynamic removal, even when the surfaces are electrostatically favorable for attachment (Torkzaban and Bradford, 2016). Consequently, only a small fraction of the collector surface can contribute to irreversible attachment due to spatial variability of roughness properties (Bradford et al., 2017). Note that the AgNP mass transfer rates to roughness pillar tops (fast) and valleys (slow) are expected to be different and this provides a potential explanation for the need to consider two retention sites. In addition, the energy barrier can be reduced and/or eliminated and the depth of the primary minimum can be increased when roughness and pore structure create valleys where AgNPs are wedged (Li et al., 2017).

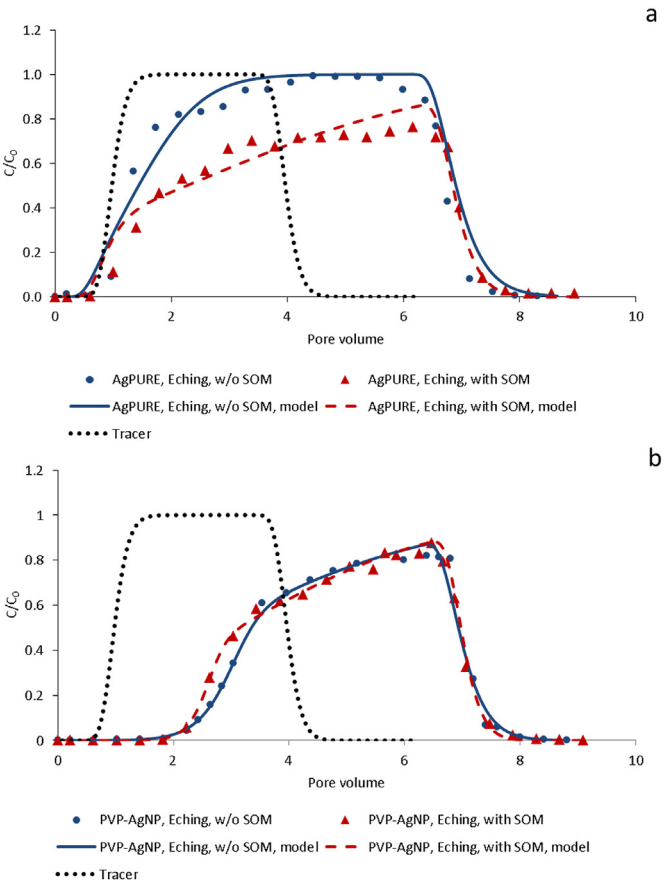

Fig. 3. Breakthrough curves of AgPURE (a) and PVP-AgNP (b) transport experiments in the presence and absence of soil organic matter (SOM) in the natural carbonate-dominated aquifer (Eching) material, respectively. Pore water velocity = 8.64 m d-1 and d50 = 0.7 mm.

Increasing amounts of chemical heterogeneity with the CCS percentage can increase the depths of the primary minimum and enhance limited attachment and wedging on these rough surfaces. The secondary minimum was always negligible (>-0.002) and was therefore not further considered. Note that the BET surface area for CCS was much larger than for quartz (Table 1), which indicates the presence of greater amounts of surface roughness and/or internal porosity.

3.3. AgNP mobility in presence and absence of SOM on carbonate-dominated aquifer material

Fig. 3 presents observed and simulated BTCs for AgPURE (Fig. 3a) and PVP-AgNP (Fig. 3b) in natural porous media in the presence and absence of SOM. Retention profiles for AgPURE and PVP-AgNP in the presence and absence of SOM are presented in the SI (Fig. S3). Table 2 summarizes the considered physicochemical conditions, measured and fitted model parameters, and mass balance information for these four transport experiments. Standard errors and confidence intervals on the fitted parameters as well as information regarding the AIC are shown in the SI (Tables S2 and S3). A summary of the replicate experiments is listed in Table S2.

The total mass recovery of AgNPs in the experiments listed in Table 2 varied between 66.3 and 99.5%. Observed AgNP BTCs were reasonably well described with the mathematical model, with R^2 ranging from 0.95 to 0.99. The AIC values indicated that blocking on a single retention site was needed to describe the BTC for AgPURE

in the absence of SOM, whereas blocking on two retention sites was needed to describe BTCs for other conditions (e.g., PVP-AgNPs in the presence and absence of SOM, and AgPURE in the presence of SOM). An example of a modeled BTC with Langmuirian blocking on one and two kinetic retention sites is presented in Fig. S5 and further information is provided in Table S2 in the SI. Bromide tracers showed a near complete recovery of 98.2–101.0%, and breakthrough close to 1 PV.

Fig. 3a indicates that the BTC for AgPURE in the absence of SOM reached unity after about 4 PV, whereas blocking was more pronounced and produced a slowly ascending plateau when SOM was present. Blocking occurs more rapidly for smaller values of S_{max} and/or S_f. The calculated value of S_f (Eq. S(5)) was very low, but more than four times higher in the presence than the absence of SOM (Table 2). Furthermore, most of the retention sites in the presence of SOM were more slowly filled than in the absence of SOM, although a smaller number filled more rapidly (Table 2). Further evidence for blocking was obtained from the RPs which showed a near uniform distribution with depth in the presence and absence of SOM (Fig. S3a). The value of the normalized solid phase concentration (S/C_0) was higher in the presence of SOM due to differences in $S_{max1}+S_{max2}$.

AgPURE exhibited higher mobility when SOM was removed from the sediments, with effluent mass recoveries of 64.9% in the presence of SOM and 87.4% in the absence of SOM (Table 2). This reflects a decrease in the adhesive interaction of AgPURE with the Eching aquifer material when SOM was removed. This can partially be explained by greater electrostatic repulsion between the AgPURE (−17.1 mV) and the sediment after the removal of SOM; e.g., the zeta potential of the soil decreased from −26.1 mV to −30.0 mV. In addition, nonionic surfactants (e.g., Tween 20) that are used to stabilize AgPURE are known to interact with SOM via various functional groups (Chiou et al., 1983; Hu et al., 2010; Urano et al., 1984). Interactions discussed in the literature that could favor increased AgNP retention on SOM-coated particles include hydrophobic interactions, hydrogen bonding or cation bridging (Baker, 1991; Grillo et al., 2015; Hoppe et al., 2014; Zhang et al., 2012; Zhang et al., 2009). Experiments with viruses showed that the presence of humic acid on silica surfaces as well as divalent cations could reduce virus mobility. It was found that calcium is capable of forming cation bridges by binding to carboxylate groups on both the humic acid and the protein shell of the virus (Pham et al., 2009).

Fig. 3b shows that the BTCs for PVP-AgNPs were similar in the presence and absence of SOM. In contrast to AgPURE (Fig. 3a), SOM only had a minor influence on the mobility of PVP-AgNPs (Fig. 3b); e.g., a breakthrough in the presence of SOM occurred slightly before that in the absence of SOM, and then reached similar plateau values. Table 2 indicates that the effluent recoveries of PVP-AgNPs were similar in the presence and absence of SOM (52.6% and 51.5%, respectively). BTCs for PVP-AgNPs in both porous media had $S_{max1}<S_{max2}$ and $k_{sw1} \gg k_{sw2}$ (Table 2). The total value of $S_{max1}+S_{max2}$ was similar in the presence and absence of SOM, but the calculated value of S_f was still very small (Table 2). RPs of PVP-AgNPs (Fig. S3b) show no clear trend, although higher Ag concentrations were determined in the presence of SOM.

The effluent mass recovery in Table 2 indicates that PVP-AgNPs exhibited less mobility than AgPURE in the Eching aquifer material without and with SOM. Consistent with these observations, the parameters k_{sw1}, k_{sw2}, S_{max1}, S_{max2}, and S_f were also larger for the PVP-AgNPs than AgPURE. These observations can be partially explained by the more negative charge for AgPURE (−17.1 mV) compared to PVP-AgNPs (−9.8 mV) in 1 mM $NaHCO_3$ at pH 8.3 (Table 1). The electrostatic repulsion between AgPURE and the aquifer material is, therefore, higher than between PVP-AgNPs and the aquifer material leading to more favorable attachment conditions for PVP-coated AgNPs. Several other factors can also contribute to differences in interactions of AgPURE and PVP-NPs with SOM. It is possible that hydrogen bonding or hydrophobic interactions that are relevant for Tween 20-binding to SOM might not be significant in the case of the polymer-SOM interactions. SOM has been found to mask charge heterogeneities and cation bridging with clay particles (Cabal et al., 2010; Han et al., 2008). The interaction of SOM with AgNPs is also expected to be sensitive to the roughness density and height of the AgNP capping agent (Bradford et al., 2017, 2018) and the bonding energy between the capping agent and the AgNP (Gunsolus et al., 2015). Additional research is warranted to determine the underlying cause for differences in SOM-AgNP interactions, but a systematic evaluation of these factors is beyond the scope of this work.

4. Conclusions

We systematically examined the fate of AgNPs in the presence of carbonate minerals. Increasing the CCS content in the artificially mixed porous medium tended to lead to greater retardation of the breakthrough curve and increasing retention of AgNPs, although AgPURE was much less affected by the CCS content than PVP-AgNPs. Interestingly, only a small portion of the solid surface area contributed to AgNP retention, even on positively charged CCS. Interaction energy calculations demonstrated that the presence of small amounts of nanoscale roughness on the CCS will dramatically weaken the adhesive interaction and can explain why only limited AgNP retention occurred on these surfaces. Consequently, the experimental and modeling results, and interaction energy calculations demonstrate that chemical heterogeneity played a secondary role in AgNP retention than nanoscale roughness. Furthermore, these experiments demonstrate that AgNP breakthrough in CCS-containing porous media mixtures depends on the AgNP stabilizing agent, the solid surface roughness, and the amount of favorable attachment places available on the porous medium. The latter is directly dependent on the CCS content that in a natural material would be defined by geological and geochemical processes.

Experiments with the natural aquifer material (Eching) showed that AgPURE is retarded in its breakthrough in the presence of SOM, whereas SOM removal had no significant impact on the retention behavior of PVP-AgNP. AgPURE interactions with SOM have been attributed to hydrophobic interactions, hydrogen bonding or cation bridging. The insensitivity of PVP-AgNP to the presence of SOM was partially attributed to a decrease in the electrostatic repulsion of PVP-AgNPs, which diminished the relative importance of hydrophobic interactions or cation bridging.

This study demonstrates the complex interplay between stabilizing agent, surface roughness and soil organic matter regarding the transport and fate of surfactant- and polymer-stabilized AgNPs in carbonate-rich porous media. Based on the information presented in this work we can predict that the transport of AgNPs in porous media with increasing carbonate content will be reduced more strongly in the case of polymer-coated than surfactant-stabilized AgNPs. In contrast, the retention of surfactant-stabilized AgNPs will be larger than that of polymer-stabilized ones in the presence of natural organic matter.

Calcium carbonate-rich sand is part of many vadose zones and aquifers used for drinking water production around the world. As such, our findings could become important for future field-scale studies related to silver nanoparticle transport in shallow unconsolidated calcareous and siliceous porous media, especially at locations where these are exposed to significant input of silver nanoparticles.

Conflict of intrest

The authors declare no competing interests.

Acknowledgments

The contributions of Yorck F. Adrian and Uwe Schneidewind were funded in part by the Federal Ministry of Education and Research (BMBF), Germany, Project Nanomobil (03X0151A). The authors would like to thank Yvonne Münchow and Bruno Köhler from RWTH Aachen University, Department of Engineering Geology and Hydrogeology for their help with some of the laboratory work and Claudia Walraf from Research Center Jülich for the BET measurements. CamSizer measurements were carried out with help of the Department of Engineering Geology at TU Berlin. TEM measurements were carried out by Nina Siebers (IBG-3) at the Ernst Ruska-Centre (ER-C), Research Center Jülich, Germany.

Appendix A. Supplementary data

Supplementary data to this article can be found online at https://doi.org/10.1016/j.envpol.2019.113124.

References

Adrian, Y.F., Schneidewind, U., Bradford, S.A., Simunek, J., Fernandez-Steeger, T.M., Azzam, R., 2018. Transport and retention of surfactant- and polymer-stabilized engineered silver nanoparticles in silicate-dominated aquifer material. Environ. Pollut. 236, 195–207. https://doi.org/10.1016/j.envpol.2018.01.011.

Akaike, H., 1974. A new look at the statistical-model identification. IEEE Trans. Autom. Control 19, 716–723. https://doi.org/10.1109/TAC.1974.1100705.

Al Mahrouqi, D., Vinogradov, J., Jackson, M.D., 2017. Zeta potential of artificial and natural calcite in aqueous solution. Adv. Colloid Interface Sci. 240, 60–76. https://doi.org/10.1016/j.cis.2016.12.006.

Baker, R.A., 1991. Organic Substances and Sediments in Water, vol. II. CRC Press.

Bäuerlein, P.S., Emke, E., Tromp, P., Hofman, J.A., Carboni, A., Schooneman, F., de Voogt, P., van Wezel, A.P., 2017. Is there evidence for man-made nanoparticles in the Dutch environment? Sci. Total Environ. 576, 273–283. https://doi.org/10.1016/j.scitotenv.2016.09.206.

Bayat, A.E., Junin, R., Ghadikolaei, F.D., Piroozian, A., 2014. Transport and aggregation of Al2O3 nanoparticles through saturated limestone under high ionic strength conditions: measurements and mechanisms. J. Nanoparticle Res. 16 https://doi.org/10.1007/s11051-014-2747-x.

Bayat, A.E., Junin, R., Mohsin, R., Hokmabadi, M., Shamshirband, S., 2015. Influence of clay particles on Al2O3 and TiO2 nanoparticles transport and retention through limestone porous media: measurements and mechanisms. J. Nanoparticle Res. 17 https://doi.org/10.1007/s11051-015-3031-4.

Becker, M.D., Wang, Y., Pennell, K.D., Abriola, L.M., 2015. A multi-constituent site blocking model for nanoparticle and stabilizing agent transport in porous media. Environ. Sci.: Nano 2, 155–166. https://doi.org/10.1039/c4en00176a.

Bendersky, M., Davis, J.M., 2011. DLVO interaction of colloidal particles with topographically and chemically heterogeneous surfaces. J. Colloid Interface Sci. 353, 87–97. https://doi.org/10.1016/j.jcis.2010.09.058.

Bhattacharjee, S., Ko, C.-H., Elimelech, M., 1998. DLVO interaction between rough surfaces. Langmuir 14, 3365–3375. https://doi.org/10.1021/la971360b.

Bradford, S.A., Kim, H., Shen, C., Sasidharan, S., Shang, J., 2017. Contributions of nanoscale roughness to anomalous colloid retention and stability behavior. Langmuir 33, 10094–10105. https://doi.org/10.1021/acs.langmuir.7b02445.

Bradford, S.A., Sasidharan, S., Kim, H., Hwang, G., 2018. Comparison of types and amounts of nanoscale heterogeneity on bacteria retention. Front. Environ. Sci. 6 https://doi.org/10.3389/fenvs.2018.00056.

Bradford, S.A., Torkzaban, S., 2013. Colloid interaction energies for physically and chemically heterogeneous porous media. Langmuir 29, 3668–3676. https://doi.org/10.1021/la400229f.

Bradford, S.A., Torkzaban, S., 2015. Determining parameters and mechanisms of colloid retention and release in porous media. Langmuir 31, 12096–12105. https://doi.org/10.1021/acs.langmuir.5b03080.

Bradford, S.A., Torkzaban, S., Simunek, J., 2011. Modeling colloid transport and retention in saturated porous media under unfavorable attachment conditions. Water Resour. Res. 47, W10503 https://doi.org/10.1029/2011wr010812.

Bradford, S.A., Wang, Y., Kim, H., Torkzaban, S., Šimůnek, J., 2014. Modeling microorganism transport and survival in the subsurface. J. Environ. Qual. 43, 421–440.

Braun, A., Klumpp, E., Azzam, R., Neukum, C., 2015. Transport and deposition of stabilized engineered silver nanoparticles in water saturated loamy sand and silty loam. Sci. Total Environ. 535, 102–112. https://doi.org/10.1016/j.scitotenv.2014.12.023.

Cabal, B., Torrecillas, R., Malpartida, F., Moya, J.S., 2010. Heterogeneous precipitation of silver nanoparticles on kaolinite plates. Nanotechnology 21. https://doi.org/10.1088/0957-4484/21/47/475705.

Chen, L., Zhang, G., Wang, L., Wu, W., Ge, J., 2014. Zeta potential of limestone in a large range of salinity. Colloid. Surf. Physicochem. Eng. Asp. 450, 1–8. https://doi.org/10.1016/j.colsurfa.2014.03.006.

Chiou, C.T., Porter, P.E., Schmedding, D.W., 1983. Partition equilibriums of nonionic organic compounds between soil organic matter and water. Environ. Sci. Technol. 17, 227–231. https://doi.org/10.1021/es00110a009.

Chu, Y., Jin, Y., Flury, M., Yates, M.V., 2001. Mechanisms of virus removal during transport in unsaturated porous media. Water Resour. Res. 37, 253–263. https://doi.org/10.1029/2000wr900308.

Clough, A., Skjemstad, J.O., 2000. Physical and chemical protection of soil organic carbon in three agricultural soils with different contents of calcium carbonate. Aust. J. Soil Res. 38, 1005–1016.

Cornelis, G., Pang, L., Doolette, C., Kirby, J.K., McLaughlin, M.J., 2013. Transport of silver nanoparticles in saturated columns of natural soils. Sci. Total Environ. 463–464, 120–130. https://doi.org/10.1016/j.scitotenv.2013.05.089.

Degenkolb, L., Metreveli, G., Philippe, A., Brandt, A., Leopold, K., Zehlike, L., Vogel, H.J., Schaumann, G.E., Baumann, T., Kaupenjohann, M., Lang, F., Kumahor, S., Klitzke, S., 2018. Retention and remobilization mechanisms of environmentally aged silver nanoparticles in an artificial riverbank filtration system. Sci. Total Environ. 645, 192–204. https://doi.org/10.1016/j.scitotenv.2018.07.079.

DIN 18123, 2011. Baugrund, Untersuchung von Bodenproben – Bestimmung der Korngrößenverteilung, Soil, investigation and testing – Determination of grain-size distribution. Deutsches Institut für Normung e.V., Berlin.

DIN 18124, 2011. Baugrund, Untersuchung von Bodenproben – Bestimmung der Korndichte – Kapillarpyknometer, Weithalspyknometer, Gaspyknometer, Soil, investigation and testing – Determination of density of solid particles – Capillary pyknometer, wide mouth pycnometer, gas pycnometer. Deutsches Institut für Normung e.V., Berlin.

DIN EN 15933, 2012. Schlamm, behandelter Bioabfall und Boden - Bestimmung des pH-Werts. Deutsches Institut für Normung e.V.

Doerr, S., Shakesby, R., Walsh, R., 2000. Soil water repellency: its causes, characteristics and hydro-geomorphological significance. Earth Sci. Rev. 51, 33–65.

Dong, S., Sun, Y., Gao, B., Shi, X., Xu, H., Wu, J., Wu, J., 2017. Retention and transport of graphene oxide in water-saturated limestone media. Chemosphere 180, 506–512. https://doi.org/10.1016/j.chemosphere.2017.04.052.

Farkas, J., Peter, H., Christian, P., Gallego Urrea, J.A., Hassellov, M., Tuoriniemi, J., Gustafsson, S., Olsson, E., Hylland, K., Thomas, K.V., 2011. Characterization of the effluent from a nanosilver producing washing machine. Environ. Int. 37, 1057–1062. https://doi.org/10.1016/j.envint.2011.03.006.

Gaffey, S.J., Bronnimann, C.E., 1993. Effects of bleaching on organic and mineral phases in biogenic carbonates. J. Sediment. Res. 63, 752–754. https://doi.org/10.1306/d4267be0-2b26-11d7-8648000102c1865d.

Grillo, R., Rosa, A.H., Fraceto, L.F., 2015. Engineered nanoparticles and organic matter: a review of the state-of-the-art. Chemosphere 119, 608–619. https://doi.org/10.1016/j.chemosphere.2014.07.049.

Gunsolus, I.L., Mousavi, M.P., Hussein, K., Buhlmann, P., Haynes, C.L., 2015. Effects of humic and fulvic acids on silver nanoparticle stability, dissolution, and toxicity. Environ. Sci. Technol. 49, 8078–8086. https://doi.org/10.1021/acs.est.5b01496.

Han, Z., Zhang, F., Lin, D., Xing, B., 2008. Clay minerals affect the stability of surfactant-facilitated carbon nanotube suspensions. Environ. Sci. Technol. 42, 6869–6875. https://doi.org/10.1021/es801150j.

Heberling, F., Trainor, T.P., Lutzenkirchen, J., Eng, P., Denecke, M.A., Bosbach, D., 2011. Structure and reactivity of the calcite-water interface. J. Colloid Interface Sci. 354, 843–857. https://doi.org/10.1016/j.jcis.2010.10.047.

Hoek, E.M., Agarwal, G.K., 2006. Extended DLVO interactions between spherical particles and rough surfaces. J. Colloid Interface Sci. 298, 50–58. https://doi.org/10.1016/j.jcis.2005.12.031.

Hoppe, M., Mikutta, R., Utermann, J., Duijnisveld, W., Guggenberger, G., 2014. Retention of sterically and electrosterically stabilized silver nanoparticles in soils. Environ. Sci. Technol. 48, 12628–12635. https://doi.org/10.1021/es5026189.

Hu, J.D., Zevi, Y., Kou, X.M., Xiao, J., Wang, X.J., Jin, Y., 2010. Effect of dissolved organic matter on the stability of magnetite nanoparticles under different pH and ionic strength conditions. Sci. Total Environ. 408, 3477–3489. https://doi.org/10.1016/j.scitotenv.2010.03.033.

Huang, W., Peng, P.a., Yu, Z., Fu, J., 2003. Effects of organic matter heterogeneity on sorption and desorption of organic contaminants by soils and sediments. Appl. Geochem. 18, 955–972.

Israelachvili, J.N., 2011. Intermolecular and Surface Forces, third ed. Academic Press, San Diego.

Johnson, W.P., Rasmuson, A., Pazmino, E., Hilpert, M., 2018. Why variant colloid transport behaviors emerge among identical individuals in porous media when colloid-surface repulsion exists. Environ. Sci. Technol. 52, 7230–7239. https://doi.org/10.1021/acs.est.8b00811.

Juganson, K., Mortimer, M., Ivask, A., Pucciarelli, S., Miceli, C., Orupold, K., Kahru, A., 2017. Mechanisms of toxic action of silver nanoparticles in the protozoan Tetrahymena thermophila: from gene expression to phenotypic events. Environ. Pollut. 225, 481–489. https://doi.org/10.1016/j.envpol.2017.03.013.

Kaegi, R., Sinnet, B., Zuleeg, S., Hagendorfer, H., Mueller, E., Vonbank, R., Boller, M., Burkhardt, M., 2010. Release of silver nanoparticles from outdoor facades. Environ. Pollut. 158, 2900–2905. https://doi.org/10.1016/j.envpol.2010.06.009.

Kaegi, R., Voegelin, A., Ort, C., Sinnet, B., Thalmann, B., Krismer, J., Hagendorfer, H., Elumelu, M., Mueller, E., 2013. Fate and transformation of silver nanoparticles in urban wastewater systems. Water Res. 47, 3866–3877. https://doi.org/10.1016/j.watres.2012.11.060.

Kaegi, R., Voegelin, A., Sinnet, B., Zuleeg, S., Hagendorfer, H., Burkhardt, M., Siegrist, H., 2011. Behavior of metallic silver nanoparticles in a pilot wastewater treatment plant. Environ. Sci. Technol. 45, 3902–3908. https://doi.org/10.1021/es1041892.

Klein, C., Comero, S., Stahlmecka, B., Romazanov, J., Kuhlbusch, T.A.J., Van Doren, E., De Temmerman, P.J., Mast, J., Wick, P., Kurg, H., 2011. NM-Series of Representative Manufactured Nanomaterials NM-300 Silver Characterization, Stability, Homogeneity. JRC Scientific and Technical Report.

Klitzke, S., Metreveli, G., Peters, A., Schaumann, G.E., Lang, F., 2015. The fate of silver nanoparticles in soil solution–Sorption of solutes and aggregation. Sci. Total Environ. 535, 54–60. https://doi.org/10.1016/j.scitotenv.2014.10.108.

Laumann, S., Micic, V., Lowry, G.V., Hofmann, T., 2013. Carbonate minerals in porous media decrease mobility of polyacrylic acid modified zero-valent iron nanoparticles used for groundwater remediation. Environ. Pollut. 179, 53–60. https://doi.org/10.1016/j.envpol.2013.04.004.

Leij, F.J., Bradford, S.A., Wang, Y., Sciortino, A., 2015. Langmuirian blocking of irreversible colloid retention: analytical solution, moments, and setback distance. J. Environ. Qual. 44, 1473–1482. https://doi.org/10.2134/jeq2015.03.0147.

Li, T., Jin, Y., Huang, Y., Li, B., Shen, C., 2017. Observed dependence of colloid detachment on the concentration of initially attached colloids and collector surface heterogeneity in porous media. Environ. Sci. Technol. 51, 2811–2820.

Liang, Y., Bradford, S.A., Simunek, J., Heggen, M., Vereecken, H., Klumpp, E., 2013a. Retention and remobilization of stabilized silver nanoparticles in an undisturbed loamy sand soil. Environ. Sci. Technol. 47, 12229–12237. https://doi.org/10.1021/es402046u.

Liang, Y., Bradford, S.A., Simunek, J., Vereecken, H., Klumpp, E., 2013b. Sensitivity of the transport and retention of stabilized silver nanoparticles to physicochemical factors. Water Res. 47, 2572–2582. https://doi.org/10.1016/j.watres.2013.02.025.

MacCarthy, P., Rice, J.A., 1985. In: Aiken, G.R., McKnight, D.M., Wershaw, R.L., MacCarthy, P. (Eds.), Humic substances in soil, sediment, and water. geochemistry, isolation and characterization. Wiley, New York, p. 275.

Maillard, J.Y., Hartemann, P., 2013. Silver as an antimicrobial: facts and gaps in knowledge. Crit. Rev. Microbiol. 39, 373–383. https://doi.org/10.3109/1040841X.2012.713323.

Makama, S., Piella, J., Undas, A., Dimmers, W.J., Peters, R., Puntes, V.F., van den Brink, N.W., 2016. Properties of silver nanoparticles influencing their uptake in and toxicity to the earthworm Lumbricus rubellus following exposure in soil. Environ. Pollut. 218, 870–878. https://doi.org/10.1016/j.envpol.2016.08.016.

Makselon, J., Siebers, N., Meier, F., Vereecken, H., Klumpp, E., 2018. Role of rain intensity and soil colloids in the retention of surfactant-stabilized silver nanoparticles in soil. Environ. Pollut. 238, 1027–1034. https://doi.org/10.1016/j.envpol.2018.02.025.

Makselon, J., Zhou, D., Engelhardt, I., Jacques, D., Klumpp, E., 2017. Experimental and numerical investigations of silver nanoparticle transport under variable flow and ionic strength in soil. Environ. Sci. Technol. 51, 2096–2104. https://doi.org/10.1021/acs.est.6b04882.

Mallevre, F., Fernandes, T.F., Aspray, T.J., 2014. Silver, zinc oxide and titanium dioxide nanoparticle ecotoxicity to bioluminescent Pseudomonas putida in laboratory medium and artificial wastewater. Environ. Pollut. 195, 218–225. https://doi.org/10.1016/j.envpol.2014.09.002.

Menzel, M., Bienert, R., Bremser, W., Girod, M., Rolf, S., Thünemann, A.F., Emmerling, F., 2013. Certified Reference Material BAM-N001 - Particle Size Parameters of Nano Silver. BAM Federal Institute for Material Research and Testing. Devision 1.3 Structure Analysis, Berlin, Germany.

Mikutta, R., Kleber, M., Kaiser, K., Jahn, R., 2005. Review: organic matter removal from soils using hydrogen peroxide, sodium hypochlorite, and disodium peroxodisulfate. Soil Sci. Soc. Am. J. 69, 120–135. https://doi.org/10.2136/sssaj2005.0120.

Morales, V.L., Gao, B., Steenhuis, T.S., 2009. Grain surface-roughness effects on colloidal retention in the vadose zone. Vadose Zone J. 8, 11–20. https://doi.org/10.2136/vzj2007.0171.

Navarro, E., Piccapietra, F., Wagner, B., Marconi, F., Kaegi, R., Odzak, N., Sigg, L., Behra, R., 2008. Toxicity of silver nanoparticles to *Chlamydomonas reinhardtii*. Environ. Sci. Technol. 42, 8959–8964. https://doi.org/10.1021/es801785m.

Neukum, C., Braun, A., Azzam, R., 2014a. Transport of engineered silver (Ag) nanoparticles through partially fractured sandstones. J. Contam. Hydrol. 164, 181–192.

Neukum, C., Braun, A., Azzam, R., 2014b. Transport of stabilized engineered silver (Ag) nanoparticles through porous sandstones. J. Contam. Hydrol. 158, 1–13.

Panacek, A., Kolar, M., Vecerova, R., Prucek, R., Soukupova, J., Krystof, V., Hamal, P., Zboril, R., Kvitek, L., 2009. Antifungal activity of silver nanoparticles against Candida spp. Biomaterials 30, 6333–6340. https://doi.org/10.1016/j.biomaterials.2009.07.065.

Park, C.M., Heo, J., Her, N., Chu, K.H., Jang, M., Yoon, Y., 2016. Modeling the effects of surfactant, hardness, and natural organic matter on deposition and mobility of silver nanoparticles in saturated porous media. Water Res. 103, 38–47. https://doi.org/10.1016/j.watres.2016.07.022.

Peters, R.J.B., van Bemmel, G., Milani, N.B.L., den Hertog, G.C.T., Undas, A.K., van der Lee, M., Bouwmeester, H., 2018. Detection of nanoparticles in Dutch surface waters. Sci. Total Environ. 621, 210–218. https://doi.org/10.1016/j.scitotenv.2017.11.238.

Pham, M., Mintz, E.A., Nguyen, T.H., 2009. Deposition kinetics of bacteriophage MS2 to natural organic matter: role of divalent cations. J. Colloid Interface Sci. 338, 1–9. https://doi.org/10.1016/j.jcis.2009.06.025.

Rahmatpour, S., Mosaddeghi, M.R., Shirvani, M., Šimůnek, J., 2018. Transport of silver nanoparticles in intact columns of calcareous soils: the role of flow conditions and soil texture. Geoderma 322, 89–100. https://doi.org/10.1016/j.geoderma.2018.02.016.

Rasmuson, A., Pazmino, E., Assemi, S., Johnson, W.P., 2017. Contribution of nano- to microscale roughness to heterogeneity: closing the gap between unfavorable and favorable colloid attachment conditions. Environ. Sci. Technol. 51, 2151–2160. https://doi.org/10.1021/acs.est.6b05911.

Rice, J.A., MacCarthy, P., 1990. A model of humin. Environ. Sci. Technol. 24, 1875–1877.

Ryan, J.N., Elimelech, M., Ard, R.A., Harvey, R.W., Johnson, P.R., 1999. Bacteriophage PRD1 and silica colloid transport and recovery in an iron oxide-coated sand aquifer. Environ. Sci. Technol. 33, 63–73. https://doi.org/10.1021/es980350+.

Sagee, O., Dror, I., Berkowitz, B., 2012. Transport of silver nanoparticles (AgNPs) in soil. Chemosphere 88, 670–675. https://doi.org/10.1016/j.chemosphere.2012.03.055.

Sasidharan, S., Torkzaban, S., Bradford, S.A., Dillon, P.J., Cook, P.G., 2014. Coupled effects of hydrodynamic and solution chemistry on long-term nanoparticle transport and deposition in saturated porous media. Colloid. Surf. Physicochem. Eng. Asp. 457, 169–179. https://doi.org/10.1016/j.colsurfa.2014.05.075.

Siller, L., Lemloh, M.L., Piticharoenphun, S., Mendis, B.G., Horrocks, B.R., Brummer, F., Medakovic, D., 2013. Silver nanoparticle toxicity in sea urchin Paracentrotus lividus. Environ. Pollut. 178, 498–502. https://doi.org/10.1016/j.envpol.2013.03.010.

Šimůnek, J., van Genuchten, M.T., Šejna, M., 2008. Development and applications of the HYDRUS and STANMOD software packages and related codes. Vadose Zone J. 7, 587. https://doi.org/10.2136/vzj2007.0077.

Šimůnek, J., van Genuchten, M.T., Šejna, M., 2016. Recent developments and applications of the HYDRUS computer software packages. Vadose Zone J. 15 https://doi.org/10.2136/vzj2016.04.0033.

Somasundaran, P., Agar, G.E., 1967. The zero point of charge of calcite. J. Colloid Interface Sci. 24, 433–440. https://doi.org/10.1016/0021-9797(67)90241-x.

Sondi, I., Bišćan, J., Vdović, N., Škapin, S.D., 2009. The electrokinetic properties of carbonates in aqueous media revisited. Colloid. Surf. Physicochem. Eng. Asp. 342, 84–91. https://doi.org/10.1016/j.colsurfa.2009.04.012.

Song, J., Peng, P.a., Huang, W., 2002. Black carbon and kerogen in soils and sediments. 1. Quantification and characterization. Environ. Sci. Technol. 36, 3960–3967.

Sposito, G., 2008. The Chemistry of Soils, second ed. Oxford University Press, New York, NY.

Suresh, L., Walz, J.Y., 1996. Effect of surface roughness on the interaction energy between a colloidal sphere and a flat plate. J. Colloid Interface Sci. 183, 199–213. https://doi.org/10.1006/jcis.1996.0535.

Tian, Y., Gao, B., Silvera-Batista, C., Ziegler, K.J., 2010. Transport of engineered nanoparticles in saturated porous media. J. Nanoparticle Res. 12, 2371–2380. https://doi.org/10.1007/s11051-010-9912-7.

Topuz, E., Sigg, L., Talinli, I., 2014. A systematic evaluation of agglomeration of Ag and TiO2 nanoparticles under freshwater relevant conditions. Environ. Pollut. 193, 37–44. https://doi.org/10.1016/j.envpol.2014.05.029.

Topuz, E., Traber, J., Sigg, L., Talinli, I., 2015. Agglomeration of Ag and TiO2 nanoparticles in surface and wastewater: role of calcium ions and of organic carbon fractions. Environ. Pollut. 204, 313–323. https://doi.org/10.1016/j.envpol.2015.05.034.

Torkzaban, S., Bradford, S.A., 2016. Critical role of surface roughness on colloid retention and release in porous media. Water Res. 88, 274–284. https://doi.org/10.1016/j.watres.2015.10.022.

Torkzaban, S., Kim, H.N., Simunek, J., Bradford, S.A., 2010. Hysteresis of colloid retention and release in saturated porous media during transients in solution chemistry. Environ. Sci. Technol. 44, 1662–1669. https://doi.org/10.1021/es903277p.

Troester, M., Brauch, H.J., Hofmann, T., 2016. Vulnerability of drinking water supplies to engineered nanoparticles. Water Res. 96, 255–279. https://doi.org/10.1016/j.watres.2016.03.038.

Tschapek, M., 1984. Criteria for determining the hydrophilicity-hydrophobicity of soils. Z. für Pflanzenernährung Bodenkunde 147, 137–149. https://doi.org/10.1002/jpln.19841470202.

Urano, K., Saito, M., Murata, C., 1984. Adsorption of surfactants on sediments. Chemosphere 13, 293–300. https://doi.org/10.1016/0045-6535(84)90136-x.

Vdović, N., 2001. Electrokinetic behaviour of calcite—the relationship with other calcite properties. Chem. Geol. 177, 241–248. https://doi.org/10.1016/s0009-2541(00)00397-1.

Wang, D., Bradford, S.A., Harvey, R.W., Gao, B., Cang, L., Zhou, D., 2012. Humic acid facilitates the transport of ARS-labeled hydroxyapatite nanoparticles in iron oxyhydroxide-coated sand. Environ. Sci. Technol. 46, 2738–2745. https://doi.org/10.1021/es203784u.

Wang, D., Jaisi, D.P., Yan, J., Jin, Y., Zhou, D., 2015. Transport and retention of polyvinylpyrrolidone-coated silver nanoparticles in natural soils. Vadose Zone J. 14 https://doi.org/10.2136/vzj2015.01.0007.

Wang, D., Su, C., Zhang, W., Hao, X., Cang, L., Wang, Y., Zhou, D., 2014. Laboratory assessment of the mobility of water-dispersed engineered nanoparticles in a red soil (Ultisol). J. Hydrol. 519, 1677–1687. https://doi.org/10.1016/

j.jhydrol.2014.09.053.
Yang, X., Lin, S., Wiesner, M.R., 2014. Influence of natural organic matter on transport and retention of polymer coated silver nanoparticles in porous media. J. Hazard Mater. 264, 161–168. https://doi.org/10.1016/j.jhazmat.2013.11.025.
Yecheskel, Y., Dror, I., Berkowitz, B., 2018. Silver nanoparticle (Ag-NP) retention and release in partially saturated soil: column experiments and modelling. Environ. Sci.: Nano 5, 422–435. https://doi.org/10.1039/C7EN00990A.
Zhang, H., Smith, J.A., Oyanedel-Craver, V., 2012. The effect of natural water conditions on the anti-bacterial performance and stability of silver nanoparticles capped with different polymers. Water Res. 46, 691–699. https://doi.org/10.1016/j.watres.2011.11.037.
Zhang, M., Bradford, S.A., Simunek, J., Vereecken, H., Klumpp, E., 2016. Do goethite surfaces really control the transport and retention of multi-walled carbon nanotubes in chemically heterogeneous porous media? Environ. Sci. Technol. 50, 12713–12721. https://doi.org/10.1021/acs.est.6b03285.
Zhang, Y., Chen, Y., Westerhoff, P., Crittenden, J., 2009. Impact of natural organic matter and divalent cations on the stability of aqueous nanoparticles. Water Res. 43, 4249–4257. https://doi.org/10.1016/j.watres.2009.06.005.